e-PS, 2010, **7**, 87-95
ISSN: 1581-9280 web edition
ISSN: 1854-3928 print edition

www.Morana-rtd.com

e-PRESERVATIONScience

published by MORANA RTD d.o.o.

FULL PAPER

PARCHMENT AGEING STUDY: NEW METHODS BASED ON THERMAL TRANSPORT AND SHRINKAGE ANALYSIS

Antonella Riccardi, Fulvio Mercuri, Stefano Paoloni, Ugo Zammit, Massimo Marinelli, Folco Scudieri

Dipartimento di Ingegneria Meccanica and Laboratorio di Conservazione e Restauro dei Beni Librari, Facoltà di Lettere e Filosofia, Università di Roma "Tor Vergata", Via del Politecnico 1, 00133 Roma, Italia

corresponding author:
fulvio.mercuri@uniroma2.it

The structure of the parchment and its preservation state have been studied by means of novel methods based on the analysis of the heat diffusion and the shrinkage activity. Investigations have been performed on modern, inked and non-inked, parchment artificially aged in different conditions, as well as on modern non-aged and historical parchment samples. By means of the infrared thermography, the thermal diffusivity D has been measured along different directions, perpendicular and parallel to the parchment leaf plane respectively, in order to characterize its anisotropy and the way it depends on ageing. Thermografic investigations have also enabled the analysis of extended micro damages induced in the parchment layered structure by the combined effect of ink and ageing. Finally, quantitative information on the degradation induced by artificially ageing have been obtained by the analysis of the hydrothermal shrinkage activity of the parchment fibres by means of a new method based on light transmission measurements.

1 Introduction

Many aspects of parchment deterioration can be related to changes occurring in the molecular structure and to the collagen fibres in particular[1]. Unfortunately deterioration cannot always be quantified by directly monitoring the phenomena occurring at the molecular scale. An alternative approach is provided by the analysis of the effects produced by the molecular transformations to the macrostructure[2]. Many physical macroscopic properties in fact reflect the collective status of the microstructure building units. Thermal transport processes, for instance, are strictly related to the kind of microstructure the heat diffuses through. In the case of the parchment the building structure are fibres and they can be considered as arranged in planes and possibly oriented, on average, along a preferable direction. Consequently the kind of structure the heat finds in its diffusion through the sample bulk is different if the propagation process is considered in the directions across ($\perp$) or along (||) the leaf plane shown in Figure 1. Therefore, it would not be surprising that such an anisotropy of the parchment

received: 4.8.2009
accepted: 4.5.2010

key words:
Parchment ageing, shrinkage temperature, thermal diffusivity, thermography

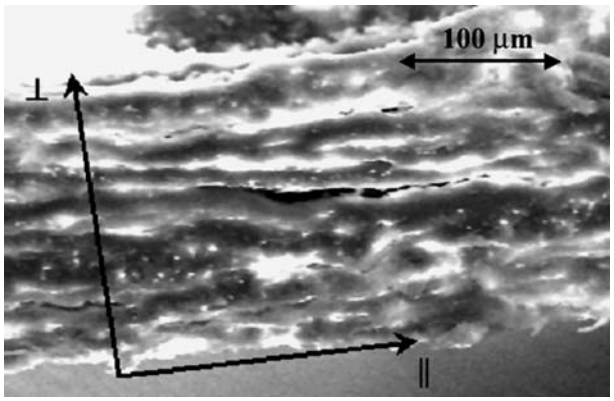

Figure 1: Scanning electron microscopy image of a parchment leaf cross-section. The arrows represent the two investigated heat diffusion directions[12].

structure can be reflected in the thermal transport properties. Such properties are also expected to depend on the preservation state of the material. Ageing conditions, in fact, can induce changes of the intra-fibres structure related to the degradation of the collagen, the main component of the parchment. In particular hydrolytic or oxidative phenomena cause the breaking of the collagen backbone chains and generate fibre cracks affecting the heat diffusion process. Under particular conditions collagen can even denature and loose its characteristic triple helix structure. Such denaturation process can be studied, in particular, by means of thermal methods[3,4,5] in structured parchment samples with different equilibrium moisture content[6] or in defibrated samples fully hydrated in *excess water* condition[3,7]. In the latter case, the macroscopic evidence of denaturation consists in the shrinkage of the collagen fibres taking place during heating[8,9]. The temperature T_S at which the fibres contraction takes place is the so called shrinkage temperature and depends on the degradation degree of the parchment. In particular, the most degraded samples denature at lower temperatures. Breaking of the collagen backbone chains, in fact, reduce the degree of hydrogen bonding among them. Consequently, the energy needed to exceed that of the hydrogen bonding is smaller in deteriorated collagen that, when heated, undergoes the transition from the triple helix structure to a randomly coiled form at lower T_S [10,11].

In the present work we propose the following novel procedures to analyse the preservation state of parchment.

One consists in the determination of the thermal diffusivity (D) along both the directions shown in Figure 1 in order to investigate the changes induced by ageing in the parchment layer structure and/or in its in-plane building units (fibres). The measurements have been performed by means of infrared thermography (IRT), a non-destructive technique which also provided infrared images for mapping and analysing extended damage produced in the parchment[13]. Such damage has also been characterized by scanning electron microscopy (SEM) and correlated to the vs. time behaviour of the IRT signal.

A second procedure consists in studying the shrinkage temperature using a new method which enables its accurate determination. The method combines the conventional polarizing microscopy observation of the shrinkage process[8,9], related to the hydrothermal denaturation of the collagen, and the quantitative analysis of the light transmitted through a portion of a defibrated sample heated in water.

2 Experimental

2.1 Thermographic determination of D

It has been recently shown that IRT can be successfully applied to the study of the structure of historical bookbindings and to the analysis of the thermal properties of the parchment, providing useful information for the evaluation of the preservation state of the material[13,14]. In particular, the thermal diffusivity D along different directions can be measured[15] in homogeneous parts of the parchment, pre-selected by IRT observations in the imaging mode. The thermal diffusivity $D_\perp$, measured along the direction perpendicular to the parchment leaf, can be obtained by means of the *pulsed* infrared thermography[16] (P-IRT) while $D_{||}$ measurements, along directions parallel to the leaf, require the *lock-in* infrared thermography[17] (L-IRT). In both cases, the heating of the parchment, induced by light absorption, is required, the consequent temperature variation being smaller than 1K.

2.1.1 Pulsed Infrared Thermography

To perform the P-IRT analysis of the parchment, one sample surface was coated by graphite so that the pulsed light produced by two flash lamps can be absorbed at the coated surface. The absorbed light induces a fast (few milliseconds) temperature rise, followed by a decay due to the heat diffusion process inside the sample. During the cooling phase, the temperature change ΔT is measured at the heated sample surface as a function of time t. By analysing the ΔT vs. t plot, we determine the so called *crossing time* τ_c , corresponding to the time it takes for the heat to cross the entire sample thickness L, which can be used for the detrmination of $D_\perp$ according to the expression[16] $D_\perp$ =

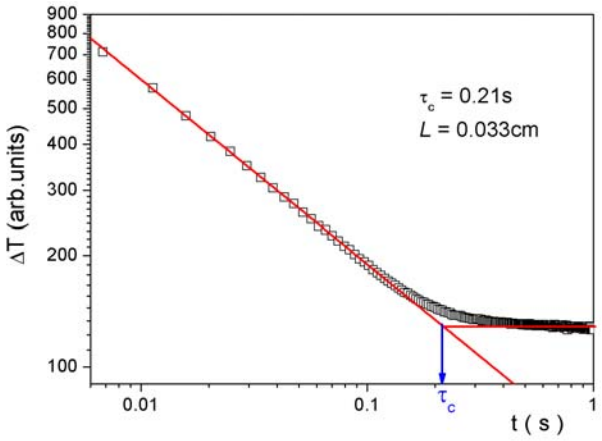

Figure 2: ΔT vs. t decay curve obtained by means of the P-IRT on the sample (M) of modern non-aged parchment of Table 1. The τ_c value obtained from the data plot has been used for the determination of $D_\perp$.

$L^2/\pi\tau_c$. As an example, Figure 2 shows the ΔT vs. t profile obtained from one of the measurements performed on the non-aged modern parchment investigated in this work. The ΔT behaviour can be briefly explained as follows. During the first part of the heat diffusion process ΔT scales as $t^{-1/2}$ therefore decreasing linearly in a log-log plot with a -0.5 slope value, as expected for an optically opaque homogeneous sample[16]. When the heat reaches the opposite surface of the leaf, it faces the thermal barrier represented by the interface with air.

The sample then tends to a thermal equilibrium state and ΔT tends to saturate to a constant value. The crossing point between these two linear regimes define the τ_c. In this case τ_c = 0.21 s and, for L = 0.33 mm, it yields to $D_\perp = 1.65 \cdot 10^{-7}$ m^2/s.

It must be pointed out that in inhomogeneous samples the profile of the decay shown in Figure 2 is no longer linear. In particular, extended defects under the surface act as thermal barriers and are responsible for the deviations from linearity as shown later on.

2.1.2 Lock-in Infrared Thermography

In this case periodic heating is produced by a modulated focused laser beam whose absorption generates a thermal wave that diffuses along the leaf plane while a synchronized IR camera detects the amplitude and the phase images of the oscillating temperature variation. Unlike the case of the P-IRT, the parchment does not need to be coated and the light is absorbed throughout the sample volume where the laser is focused. The temperature change ΔT is then studied as a function of the lateral distance d from the source point.

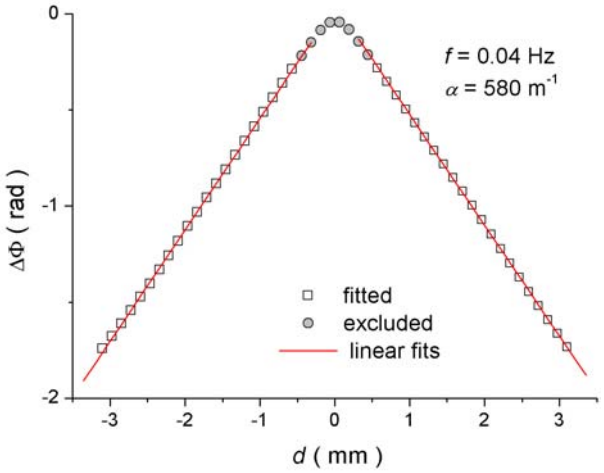

Figure 3: $\Delta\Phi$ vs. d curve obtained by means of the lock-in infrared thermography on the sample (M) of modern non-aged parchment of Table 1. The obtained slope α value has been used for the $D_{||}$ determination.

From the phase image, for d much larger than the laser spot size, $D_{||}$ can be obtained by determining the slope $\alpha = (\pi f/D_{||})^{-1/2}$ of the asymptotic linear dependence $\Delta\Phi(d) = \alpha\, d$ of the phase change with lateral distance, where f is the modulation frequency[17]. Figure 3 shows the $\Delta\Phi$ vs. d behaviour obtained with the same modern parchment sample corresponding to the results of Figure 2. In this case $\alpha = 580$ m^{-1} and, with f = 0.04 Hz, one obtains $D_{||} = 3.7 \cdot 10^{-7}$ m^2/s.

2.2 Optical determination of T_S

In order to characterize the preservation state of the analysed parchment, we studied its shrinkage activity related to the hydrothermal denaturation of collagen. Shrinkage of defibrated parchment in water is commonly studied by simple microscope observation[8,9]. We have combined such a kind of investigation with a simultaneous quantitative light transmission analysis for the shrinkage temperature determination.

The adopted experimental setup is sketched in Figure 4. The sample is contained in a quartz cell placed in a oven with automatic temperature control providing stable heating rate ranging from 0.5 mK/min to 2 Kmin. An intensity modulated laser beam passes through the sample. Part of the beam is scattered or absorbed by the parchment fibres and the remaining part is transmitted unaffected through the water. The emerging light intensity, detected by a photodiode, generates an a.c. signal which is analysed by means of a lock-in amplifier and proves to be very sensitive to changes of the fibrous network thus monitoring the shrinkage process from the very beginning.

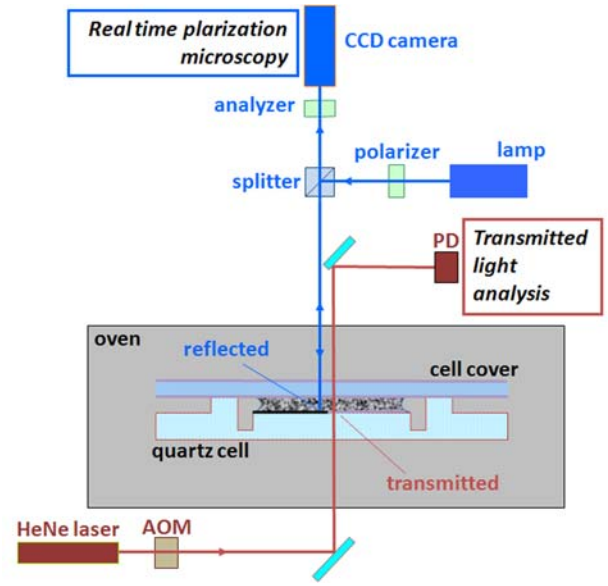

Figure 4: Experimental setup. Main components: i) heating stage including an oven containing the sample cell; ii) light transmission stage consisting of a Helium-Neon (HeNe) laser beam modulated by an Acousto-Optical Modulator (AOM), and the Photo-Detector (PD); iii) polarization microscopy system including a CCD camera.

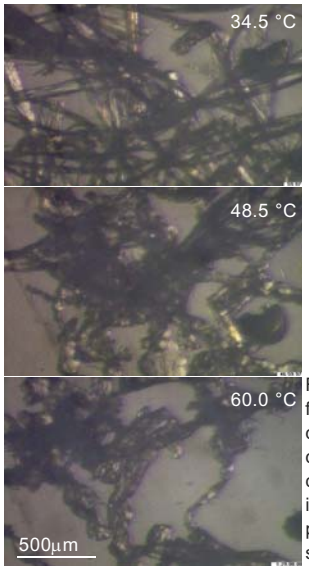

Figure 5: Picture of parchment fibres absorbed in water taken during the denaturation process at different temperature by a video camera integrated with the polarization microscopy system and providing real time images of the sample texture.

The amplitude S of the output electrical signal is recorded as a function of the temperature T simultaneously with the images of the sample texture collected by a CCD camera integrated with the experimental setup (Figure 5). The curve of Figure 6a, obtained on the same sample reported in Figures 2 and 3, shows the relative variation

$S_R(T) = [S(T) - S_0]/[S_{max} - S_0]$ of $S(T)$, where S_0 and S_{max} are, respectively, the stationary values of the signal below and above the shrinkage transition range whose temperature boundaries have been indicated in Figure 6a by the two dashed lines. The temperature profile of S_R, shown in Figure 6a, can be interpreted as follows.

The signal remains constant throughout the initial part of the measurement, where there is no movement of the fibres. When the fibres begin to shrink, a slight increase in the optical signal is observed, followed by a steep variation upon further heating until saturation occurs. That is due to different phenomena. While shrinking, the parchment fibres, that miss their hierarchical structure turning into gel, make the geometrical transmission of the sample increase, as shown in Figure 5, and reduce their ability to scatter the light[18,19,20]. The shrinkage temperature T_S is the temperature where the maximum rate of the shrinkage activity takes place. In our method, it corresponds to the flexing point of the S_R curve and, consequently, to the peak in the curve of its derivative $\dot{S}_R$ reported in Figure 6b which can be addressed as the *shrinkage temperature rate*.

Furthermore, the width of the $\dot{S}_R$ peak, similarly to the one of other physical quantities like, for example, the specific heat[3,5,6], provides us with an indication of the average degradation homogeneity throughout the sample.

The less the homogeneity the wider the temperature range over which the shrinkage occurs. Such an aspect is quantified by the value of $\Delta T_{½}$, the width at half high of the $\dot{S}_R$ peak, shown in Figure 6b.

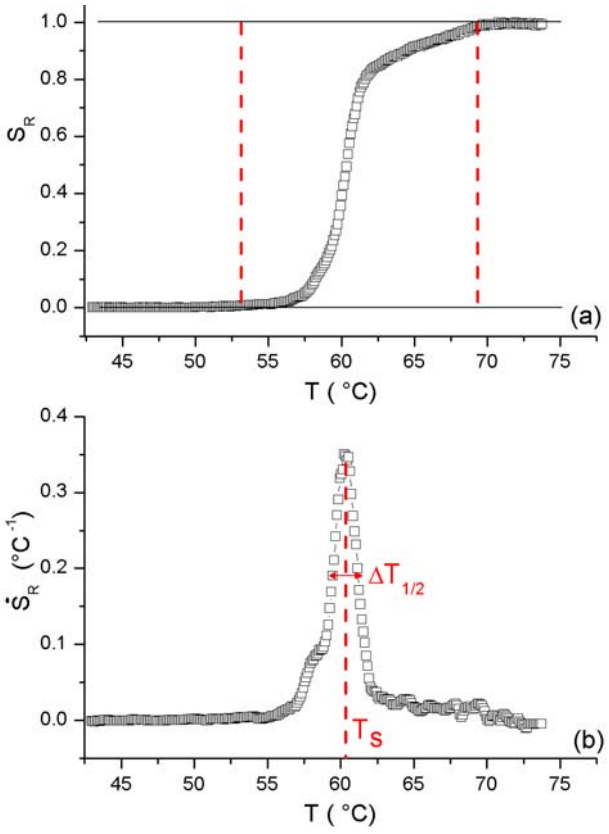

Figure 6: Modern non-aged parchment sample of table 1. a) Relative optical signal amplitude Vs. temperature. Dashed lines delimitate the transition region. b) Relative optical signal derivative: temperature position of the peak corresponds to the shrinkage temperature T_S, while the width at half high of the peak $\Delta T_{½}$ is indicative of the degree of the homogeneity of parchment degradation state.

The reported analysis is based on quantitative measurements and provides an unambiguous way to detect the onset and the evolution of the shrinkage activity, unlike from other methods based on the mere microscopic sample observation during heating. We would like to remark that the present method relies on measurements performed on a cell area of a few millimetres where a large number of fibres are present and therefore provides an average evaluation in the sample. Finally it is worthwhile noticing that, thanks to the real time polarization microscopy integrated in the experimental set up, images like the ones of Figure 5 can be collected while the light transmission measurements are being performed and associated to the optical signal evolution.

Sample	Ageing (*T=80 °C, RH=65%*)	$D_{\|\|}$ (10^{-7} m^2/s)	$D_{\perp}$ (10^{-7} m^2/s)	L (μm)	T_s (°C)
M (*)	non-aged	3.7±0.3	1.64±0.15	390±5	60,25 °C
1	2 days	4.3±0.3 (3.6±0.3)	0.75±0.15 (0.96±0.15)	305±5 (310±5)	49,60 °C
2	7 days	2.9±0.3 (3.0±0.3)	0.77±0.15 (0.94±0.15)	330±5 (355±5)	48,08 °C
3	14 days	3.4±0.3 (3.1±0.3)	0.76±0.15 (0.96±0.15)	325±5 (360±5)	45,65 °C
4	21 days	3.2±0.3 (3.1±0.3)	0.77±0.15 (0.95±0.15)	325±5 (330±5)	44.20 °C
H (**)	-				50,10 °C

Table 1: Shrinkage temperature (T_S) and thermal diffusivity (D) values as a function of ageing time. $D_{\perp}$ and $D_{||}$ refer to the values measured *along* (||) and *across* (⊥) the parchment leaf respectively. Between brackets the values obtained for the corresponding inked samples. The thickness (L) of each measured sample is also reported. The reported D and L values and the corresponding uncertainties are, respectively, the arithmetic mean of ten different measurements and twice the experimental standard deviation of the mean. *Modern (M) parchment sample comes from a leaf different from the one of the aged samples. **(H) data refers to a historical well preserved parchment.

3 Results and discussion

We have analysed two different sets of modern aged parchment samples made from the same patch of calf skin. They have been prepared at the laboratories of the National and University Library and at the Faculty of Chemistry and Chemical Technology of the University of Ljubljana. One set of samples were homogeneously inked on one side by iron gall ink while a second set was ink-free. Sample from each set have been artificially aged at 80 °C, 65% (RH) and numbered according to the scheme reported in the first two columns of Table 1 where are also reported the data corresponding to samples of non-aged modern parchment and historical parchment. However, since a non-aged sample from the same leaf as the aged ones was unavailable, one from a different leaf was used for this study.

3.1 Thermal anisotropy study

The thermal diffusivity values measured along both the investigated directions are reported in Table 1. It should be remarked that even if the modern parchment sample is supposedly homogeneous with the other ones (same animal kind, similar manifacturing, thickness, etc.), its thermal diffusivity values show marked difference with respect to those of the artificially aged samples. The thermal diffusivity is in fact strongly dependent on the specific structure of each parchment leaf and the values in Table 1 are reported as purely indicative of the general anisotropic character of such a quantity but cannot directly be compared with the ones belonging to another parchment leaf. Consequently the discussion hereby presented on the deterioration progressively induced by ageing will be based on the relative analysis of the artificially aged samples only.

The most relevant aspect shown by the data of Table 1 is that the $D_{||}$ values are about three times larger than the corresponding $D_{\perp}$ ones for both the inked and the non-inked sets of samples. Such a thermal transport anisotropy indicates that the heat diffusion process is more efficient within the planes microstructure, where the fibres of the network are tightly interconnected, than across the planes where the thinning out of the fibres connective network between adjacent layers acts as thermal barrier and is responsible for the thermal resistance in the material.

Concerning the effect of ageing on the thermal diffusivity, it can be noted that $D_{||}$ after an initial decrease tends to stabilize. On the contrary $D_{\perp}$, and therefore the heat diffusion across the planes, does not seem to be affected by ageing even at the early stage of the process when $D_{||}$ decreases. This suggests that no meaningful change occurs with ageing in the structure in between the fibre planes governing the thermal transport across the leaf while the increase of damage like fibre breaking can increase the thermal barriers concentration along the fibre planes decreasing the thermal transport efficiency in that direction. It should be pointed out that similar anisotropic behaviour of the thermal diffusivity has also been previously observed by the authors on other differently preserved samples of historical parchment. For such historical parchments the measured values of $D_{\perp}$, ranging from $0.9 \cdot 10^{-7}$ m^2/s to $1.3 \cdot 10^{-7}$ m^2/s, does not significantly differ from those of the artificially aged modern one, while the values of $D_{||}$, ranging from $1.5 \cdot 10^{-7}$ m^2/s to $3.0 \cdot 10^{-7}$ m^2/s, are sometimes considerably smaller, in particular for the most

deteriorated samples therefore suggesting that the deterioration processes makes parchment thermal transport properties progressively more isotropic.

3.2 Damage analysis of inked parchment

The thermal diffusivity values reported in bracket in Table 1 are those obtained for the inked samples. The behaviour as a function of ageing of both $D_{\perp}$ and $D_{||}$ does not substantially differ from the ones of the non-inked samples. Nevertheless, inked samples showed macroscopic ageing effects that could not be observed in the ink-free samples. In particular, the combined action of ink and ageing produced a characteristic curling of the leaf, the concave side being the inked one, and the onset of crack lines on the inked surface. In order to relate such macroscopic effects to the microstructure features, the samples were analysed by means of SEM which provided topographic images, from secondary electrons, of the leaf inked surface and cross section. The images revealed extended damage in the parchment microstructure whose distribution could be detected also by the thermographic imaging analysis.

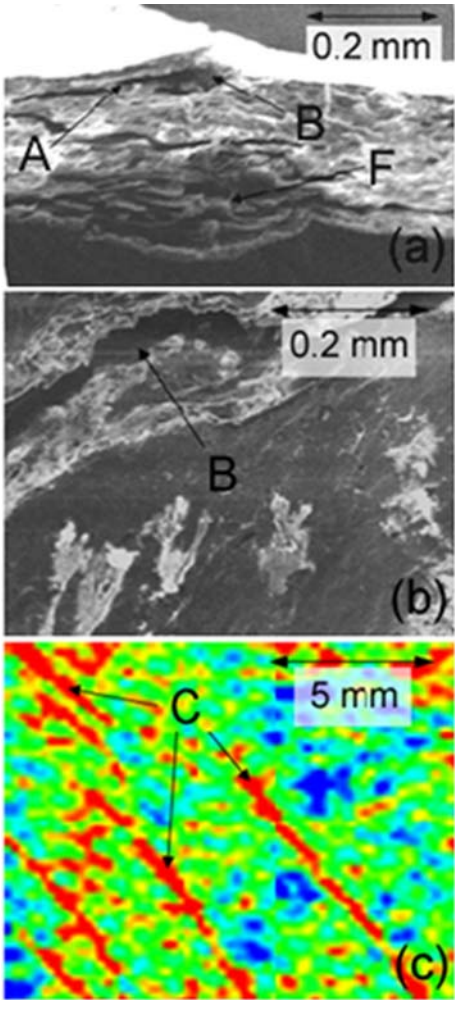

Figure 7: Sample 4 in Table 1, inked on one side. a) SEM cross-section of the parchment leaf: the inked surface is the upper one. b) SEM top view of the inked surface. c) Thermogram of the inked surface: red slanting stripes correspond to the detachment paths under the inked surface along the crack lines[12].

In Figure 7a an image of the cross-section of the inked sample 4, is reported, the inked surface being the one at the top. The image shows an extended detachment (A) just below the upper inked surface ending with a crack line (B) which is also evident in the corresponding top view reported in Figure 7b. Subsurface detachments like the A one in Figure 7a, extend below the entire observed inked area as shown by the thermogram in Figure 7c. The thermogram shows the peculiar striped features (C) characterizing the detachment areas under the inked surface generally observed around the crack line path. It can be noted that while the SEM top view image is able only to show locally the gap (B) between the two edges of the damage line separated by tenths of microns, the thermogram provides a map corresponding to a macroscopic view of the *subsurface* damage distribution. The damage appears as stripes (C) whose width, of the order 0.1 to 1 mm, corresponds to the extension of the detachment sections. In Figure

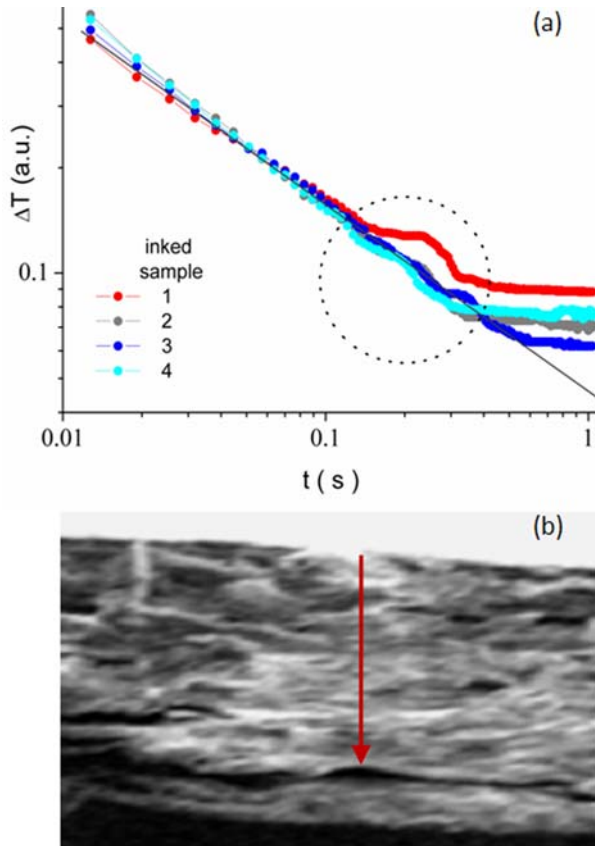

Figure 8: a) Temperature decay plot obtained at the inked surface illuminated by the flash lamps from the thermographic sequences for the four differently aged inked samples reported in Table 1. b) SEM cross section of sample 4. The arrow indicates an extended detachment causing the thermal barrier that originates the shoulder structure circled in the plot. Such a kind of features has been shown in all the analysed aged samples.

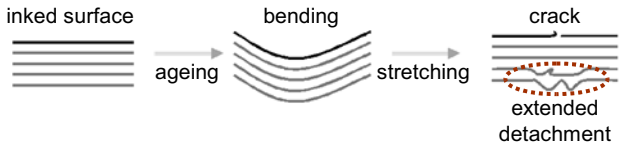

Figure 9: Sketched steps of the damage generation process.

7a, flaking (F) of the layered structure next to the non-inked surface of the parchment, from which an extended detachment propagates, is observed at the position of the crack lines (B).

In Figure 8a the temperature decay with time recorded by P-IRT at the inked surface for all the investigated inked samples, is reported. The linear decay in log-log plot shown initially by all the curves corresponds to the heat diffusion from the inked surface across the part of the sample section without extended defects. Deviations from linearity (circled peaks in the figure) reveals the presence of thermal barriers (detachments like the one pointed by the arrow in Figure 8b). Their position on the time axis is related to the depth at which they are located. They are close to the end of the decay line indicating that the position of the extended detachment is close to the opposite (non-inked) surface of the sample. It is worth to stress that, according to the model adopted for the analysis of the obtained curves, the linear behaviour shown at small t values corresponds to the heat diffusion across a homogeneous sample. That means in the present case that the connective fibres network characterizing the parchment microstructure is uniformly distributed along the investigated direction. Extended defects represent inhomogeneities and act as a thermal barrier when their size is much larger than average pore size of the microstructure. As to the origin of the above described damage, we propose the following scenario as to the process leading to the onset of the above described damages, summarized according to the sketch reported in Figure 9.

Ink is responsible for an intense shrinkage which produces the bending of the leaf. Subsequent stretching of the parchment, even by simple handling, enhances the damage producing cracks at one surface and detachments on the opposite surface where the stretched fibres are no longer able to restore their initial extended configuration.

3.3 Shrinkage temperature analysis

The shrinkage analysis has been performed on the same samples investigated by IRT in order to assess their preservation state and compare it with the thermal diffusivity analysis. In addition we have also analysed samples of modern non-aged parchment and of historical parchments. The corresponding results have been compared with those obtained from the artificially aged parchment.

The T_S values reported in Table 1 have been obtained from the vs. T profiles of the shrinkage temperature rate $\dot{S}_R$ shown in Figure 10a for the various samples. Such T_S values have been plotted in Figure10b where it is shown that they progressively decrease with the sample ageing. Such a monotonic decrease can be interpreted as an index of the increasing degree of average degradation induced in the parchment. As expected, the shrinkage temperature of the non-aged modern parchment is much larger than the others and denotes its better preservation state. The T_S value of the historical parchment is close to the one obtained for the parchment artificially aged for 2 days, revealing similar preservation conditions.

In order to compare, the dependence of T_S and $D_{||}$ on ageing, in Figure10b the $D_{||}$ values of Table 1 for artificially aged samples have been also reported where it can be envisaged that in the studied range $D_{||}$ is less sensitive to ageing than T_S. Moreover it suggests a possible non-monotonic

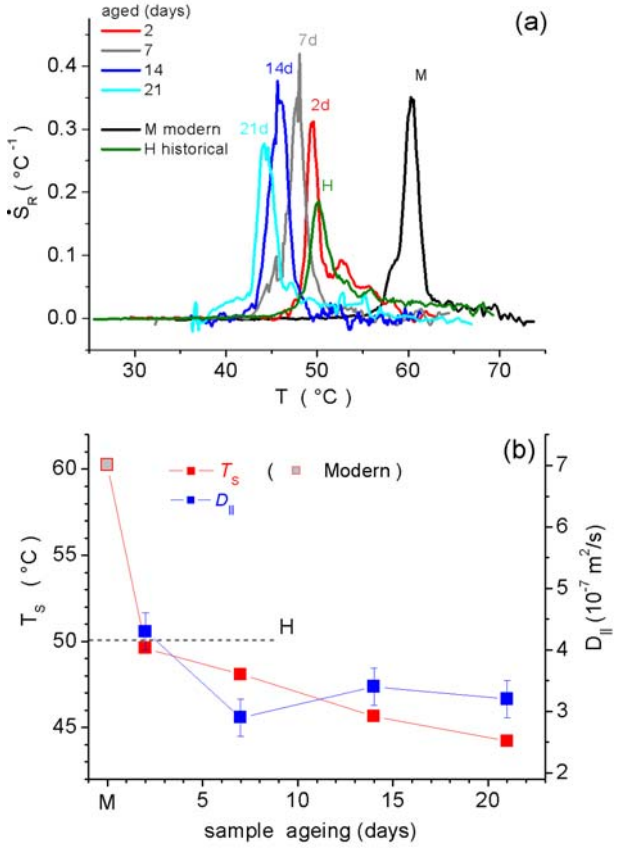

Figure 10: a) Shrinkage temperature rate $\dot{S}_R$ for the different analyzed samples obtained as the temperature derivative of the corresponding optical signal amplitude.. b) T_S and $D_{||}$ values for the different analyzed samples. Dashed line indicates the T_S value for historical (H) parchment. Modern (M) parchment sample is from a different patch and the relative data are purely indicative.

behaviour of $D_{||}$. In fact, in spite of the data showing partial superposition of the error bars, the 7 days aged sample showed $D_{||}$ values systematically smaller than the other ones. Even if the reasons for such behaviour are not clear yet, it was excluded that it could be ascribed to an unexpected higher degree of degradation of that sample because of the corresponding monotonic change of T_S vs. ageing. From the curves of Figure 10a it can be noted that the peaks of the artificially aged samples show similar $\Delta T_{½}$ widths. This reflects the homogeneous way the artificial ageing procedure acts throughout the sample volume. In other words, while the average amount of damage increases with increasing ageing, as shown by the decrease of T_S, the spectrum of the induced damage evolves rather uniformly with no meaningful relative variation of the peak width.

In this regard, it is worth to note that the above results concern the average deterioration of the analysed parchment fibres and no indication about the space distribution of the damage is provided by the employed opto-thermal investigation. Nevertheless, specific space distribution of the deterioration along a given sample direction, in particular across the parchment leaf section, can be induced by ageing, ink and surface treatments. In would be useful to study such deterioration profile but unfortunately it cannot be revealed by means of the methods proposed in this work. In fact, the T_S analysis is performed in a destructive way by evaluating, in a water suspension, samples of parchment fibres dismantled from their original texture. Concerning the IRT measurements, in both the pulsed and the lock-in configuration, they only provide information averaged over the heat propagation length where the IRT signal is generated. In this regard it must be mentioned that a number of high resolution techniques have been recently proposed providing information on the space distribution of the damage. Methods like the micro Computer Tomography (μ-CT), the micro X-ray Diffraction (μ-XRD) and the Optical Coherence Tomography (OCT), for instance, have been applied to the analysis of the microstructure degradation throughout the cross section profile of parchments and of other writing supports like paper and papyrus[20,21,22] .

4 Conclusions

The preservation state of parchment as a function of ageing has been assessed by the measurement of shrinkage temperature performed by means of a novel proposed method based on analysis of the light transmitted through the sample and studied by the measurement of thermal diffusivity performed by the IRT. The anisotropy of the parchment thermal diffusivity has been shown to be affected by ageing, reflecting deterioration processes of the microstructure that progressively make the parchment thermally more isotropic. Investigation performed on both one-side-inked and non-inked samples provided similar results. Nevertheless in the inked samples ageing induced geometry change (curling) associated to the onset of extended damages of the fibrous structure. This features have been successfully investigated by means of the IRT which provides both quantitative local information on the thermal diffusivity values and extended maps (thermograms) of the macroscopic defect distribution in the sample. The characteristic shape and extension of such defects have been also investigated by SEM. Finally the observed behaviour of the shrinkage temperature well describe the increasing degree of average degradation induced in the parchment by ageing. The analysis of light transmission profiles, characterizing the shrinkage activity of the parchment fibres, shows that the spectrum of the induced degradation evolves uniformly with the artificial ageing.

5 Acknowledgments

The authors wish to thank Jana Kolar, from the Laboratory for Cultural Heritage of the National and University Library of Ljubliana and Matija Strlič from Centre for Sustainable Heritage, The Bartlett School for Graduate Studies, University College London, UK, for processing and providing the samples and Gianluca Verona Rinati, from the Department of Mechanical Engineering of the University of Rome “Tor Vergata” for his support in the SEM analysis.

6 Literature

1. C.J. Kennedy, T.J. Wess, *The structure of Collagen within Parchment*, Restaurator, 2003, **24**, 61-80.

2. R. Larsen, D.V. Poulsen, M. Odlyha, K. Nielsen, J. Wouters, L. Puchinger, P. Brimblecombe, D. Bowden, *The use of complementary and comparative analysis in damage assessment of parchment* in: R. Larsen (ed.), *Microanalysis of parchment*, Archetype Publications, London, 2002, 165-180.

3. E. Badea, L. Miu, P. Budrugeac, M. Giurginca, A. Masic, N. Badea, G. Della Gatta, S*tudy of deterioration of historical parchments by various thermal analysis techniques complemented by SEM, FTIR, UV–VIS–NIR and unilateral NMR investigations*, J. Therm. Anal. Calorim., 2008, **91**, 17-27.

4. P. Budrugeac, L. Miu, V. Bocu, F.J. Wortman, C. Popescu, *Thermal degradation of collagen-based materials that are supports of historical objects*, J. Therm. Anal. Calorim., 2003, **72**, 1057-1064.

5. P. Budrugeac, E. Badea, G. Della Gatta, L. Miu, A. Comanescu, A *DSC study of deterioration caused by environmental chemical pollulants to parchments, a collagen-based material*, Thermochim. Acta, 2010, **500**, 51-62.

6. G. Della Gatta, E. Badea, R. Ceccarelli, T. Usacheva, A. Masic, S. Coluccia, *Assessment of damage in old parchment by DSC and SEM*, J. Therm. Anal. Calorim., 2005, **82**, 637-649

7. C. Chahine, *Changes in hydrothermal stability of leather and parchment with deterioration: a DSC study*, Thermochim. Acta, 2000, **365**, 101-110.

8. R. Larsen, M. Vest, K. Nielsen, *Determination of hydrothermal stability (Shrinkage Activity) of historical leathers measured by the micro hot table technique,* J. Soc. Leath. Tech. Ch., 1993, **77**, 151.

9. R. Larsen, D.V. Poulsen, M. Vest, *The hydrothermal stability (Shrinkage Activity) of Parchment measured by the Micro Hot Table Method (MHT)* in: R. Larsen (ed.), *Microanalysis of parchment*, Archetype Publications, London, 2002, 55-62.

10. B.H. Haines, *Collagen: the leather making protein*, in: M. Kite, R. Thomson (eds.), *Conservation of leather and related material*, Elsevier, Bruxelles, 2006, 4-10.

11. M.E. Florian, *The Mechanism of Deterioration in Leather*, in: M. Kite, R. Thomson (eds.), *Conservation of leather and related material*, Elsevier, Bruxelles, 2006, 36-57.

12. F. Mercuri, F. Scudieri, S. Paoloni, U. Zammit, M. Marinelli, *Analysis of parchment bookbinding by infrared termography*, in: M. Drdacky, M. Chapuis Eds., Proccedings of the 7th European Conference "Sauveur", Safguarded Cultural Heritage, Understanding & Viability for the Enlarged Europe, vol. 2, Prague, 2006, 755-777.

13. G. Colombo, F. Mercuri, F. Scudieri, U. Zammit, M. Marinelli, R. Volterri, *Thermographic analysis of parchment bindings*, Restaurator, 2005, **26**, 92-104.

14. M. Marinelli, F. Mercuri, F. Scudieri, U. Zammit, G. Colombo, *Thermographic study of microstructural defects in deteriorated parchment sheets*, J. Phys. IV, 2005, **125**, 527-529.

15. X.P.V. Maldague, *Theory and Practice of Infrared Technology for Non Destructive Testing*, in: K. Chang (ed.), *Wiley Series in Microwave and Optical Engineering*, John Wiley and Sons, New York, 2001.

16. F. Scudieri, F. Mercuri, R. Volterri, *Non-invasive analysis of artistic heritage and archeological findings by time resolved IR thermography*, J. Therm. Anal. Calorim., 2001, **66**, 307-314.

17. S. Paoloni, M.E. Tata, F. Scudieri, F. Mercuri, M. Marinelli, U. Zammit, *IR thermography characterization of residual stress in plastically deformed metallic components*, Appl. Phys. A, 2010, **98**, 461-465.

18. R. Reed, *Ancient Skins, Parchments, and Leathers*, Seminar Press, New York, 1972.

19. C.S. Woods, *The conservation of parchment*, in: M. Kite, R. Thomson (eds.), *Conservation of leather and related material*, Elsevier, Bruxelles, 2006, 200-224.

20. M. Góra, M. Pircher, E. Götzinger, T. Bajraszewski, M. Strlic, J. Kolar, C.K. Hitzenberger, P. Targowski, *Optical Coherence Tomography for Examination of Parchment Degradation*, Laser Chem., 2006, **2006**, 1-6.

21. R. Baumann, D. Carr Porter, W. Brent Seals, *The use of micro-CT in the study of archaeological artefacts*, in: *Art 2008* - Proceedings of the 9th International Conference on NDT of Art, Jerusalem, 2008, 1-9.

22. C.J. Kennedy, J.C Hiller, D. Lammie, M. Drakopoulos, M. Vest, M. Cooper, W.P. Adderley, T.J. Wess, *Microfocus X-Ray Diffraction of HistoricalParchment Reveals Variations in Structural Features through Parchment Cross Sections*, Nano Lett., 2004, **4**, 1373-1380.